

Construction of invariant tori around closed orbits

Mikko Kaasalainen

NORDITA, Blegdamsvej 17, 2100 Copenhagen, Denmark

Accepted 1995 February 20. Received 1994 December 19

ABSTRACT

The approach and methods introduced by McGill & Binney and Kaasalainen & Binney (Papers I and III), for the construction of phase-space tori that are approximate invariant tori of a given Hamiltonian, are generalized to include motion ‘trapped’ around general closed orbits. This is accomplished by introducing point transformations that map the configuration space around a closed orbit in the target potential to one in a toy potential for which action-angle coordinates are known. This approach opens up the possibility of constructing tori for an arbitrary orbit family. The method is illustrated by applying it to the ‘banana’ and ‘fish’ minor-orbit families in the planar logarithmic potential.

Key words: celestial mechanics, stellar dynamics – galaxies: kinematics and dynamics.

1 INTRODUCTION

In McGill & Binney (1990, Paper I), Binney & Kumar (1993, Paper II), Kaasalainen & Binney (1994a, Paper III), and Kaasalainen (1994, Paper IV), it was shown how approximate orbital tori can be constructed for a general gravitational Hamiltonian H , and how these tori can be used to define an integrable Hamiltonian H_0 that closely approximates H . The methods were applied to major-orbit families in planar as well as axisymmetric three-dimensional potentials. Secular perturbation theory was then used to treat minor-orbit families as ones made up of orbits trapped by resonances of H_0 .

Each minor-orbit family possesses its own invariant tori: they are tori of a new type in the sense that they cannot be formed by the continuous deformation of tori of H_0 . However, these ‘minor’ invariant tori are topologically similar to the ‘major’ ones in that each can be labelled with actions J_i and equipped with conjugate angle variables – for example, Binney & Spergel (1984) determined actions for tori of the ‘banana’ minor-orbit family of the logarithmic potential. Therefore, one should be able to construct these tori numerically in the same way that tori are constructed for the major-orbit families. In fact, from the geometric point of view, the division into minor- and major-orbit families is somewhat superfluous. For example, the loop orbits in a planar potential belong to a major-orbit family, but otherwise, in a Poincaré surface of section, their invariant curves look like any islands around the single point(s) of a closed orbit. Moreover, often the sobriquet ‘minor’ is inappropriate: families of low-order resonances can occupy huge portions of phase space, especially in strongly barred potentials (see, e.g., the surface of section in Fig. 3). Indeed, in the singular logarithmic potential the major family of boxes vanishes, and the entire phase space is occupied by loops and the ‘boxlet’ minor-orbit families (Miralda & Schwarzschild 1989).

The torus-construction scheme of Papers I–IV proceeds by numerically constructing the generating function of a canonical transformation that maps the invariant tori of some ‘toy’ Hamiltonian H_T (in practice that of the harmonic oscillator or the isochrone potential) into the phase space of the given ‘target’ Hamiltonian H . As discussed in Paper III, an additional canonical transformation (a point transformation) has to be introduced to make the scheme generally applicable. This is not just a matter of convenience, but absolutely essential in the case of fitting tori to loop orbits with small J_i , i.e., orbits that are so narrow and so elliptical that a circle cannot be inscribed within them. Such orbits violate the topological requirement for the generating function approach to work, mentioned in Paper I: a closed toy orbit has to fit inside the target orbit. If this does not happen in the simplest formulation of the problem, a point transformation must be introduced to deform the closed toy orbit until it does fit inside the target orbit.

Closed orbits in target potentials have infinitely many different shapes, often very complicated ones. Therefore, this paper seeks a generalized point transformation such that one can construct the invariant tori associated with any closed orbit. What is more, the motion of the orbits of a minor-type family is either librating (e.g., the banana orbits) or circulating (e.g., the fish orbits), just like with box and loop orbits, so the harmonic oscillator H_H and the isochrone H_I are natural choices for the toy Hamiltonians in this case also.

The paper is organized as follows. In Section 2 the principle of constructing a suitable coordinate system around a closed orbit is presented. With such a coordinate system one can then define a point transformation that mediates between the toy and target spaces. In Section 3 the method is applied to the banana and fish families; with the latter it is demonstrated that also an orbit crossing itself can be straightened out by a point transformation. The conclusions are presented in Section 4. A summary of a useful method of obtaining the

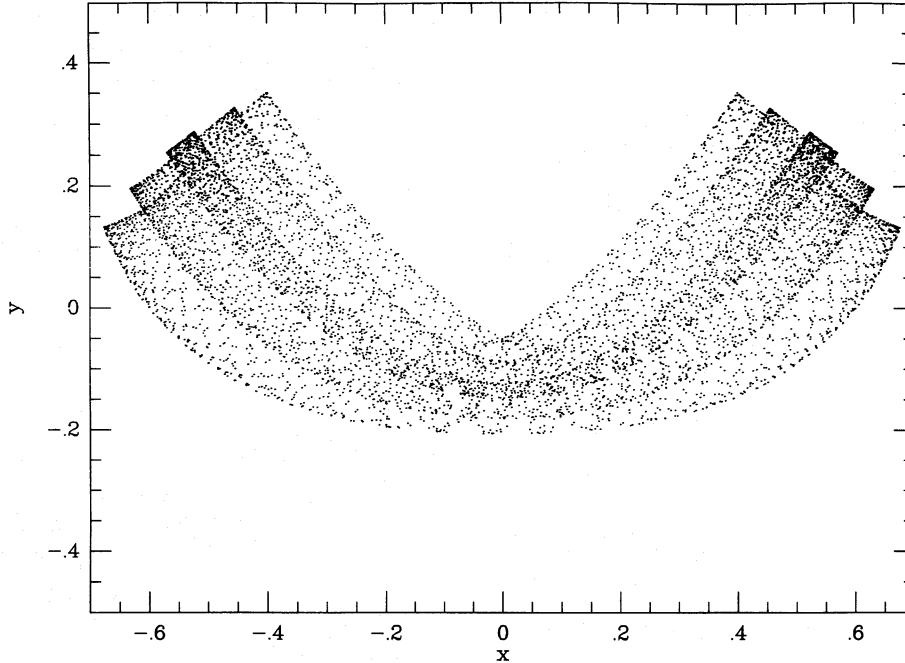


Figure 1. Three superposed banana orbits in the logarithmic potential at $R_c = 0.14$, $q = 0.6$ and $H = -0.3215$.

generating function for a torus from orbit integration is given in an appendix.

2 COORDINATE SYSTEMS AND POINT TRANSFORMATIONS FOR CLOSED ORBITS

As in Papers I–III, we employ the convention that primed variables relate to tori in the target Hamiltonian H , while the unprimed ones correspond to tori in the toy Hamiltonian H_T . The principle of our approach is first to define a point transformation such that a closed orbit in H_T is mapped to the closed orbit in H . After this, one can use the torus-fitting scheme as in Papers I–IV, provided that the target tori and the transformed toy tori are of similar types.

For a closed orbit, one of the coordinates in the toy configuration space is fixed and the value of the corresponding action J_i is zero. When $J_i > 0$, the variations in the i th coordinate describe transversal motion around the closed orbit. Correspondingly, it would be good to use a similar ‘local’ coordinate system in the target configuration space, where one coordinate always gives, in a specified manner, the distance to the chosen closed orbit. In other words, we need a coordinate system such that, under a point transformation, motion in a toy Hamiltonian projects to that around a closed orbit in the target Hamiltonian in a natural way. In general, coordinate systems like Cartesian or polar ones in the target space are not useful in this sense. (In the cases of boxes and loops they are usable because of the simple shapes of the orbits.)

The banana orbits in the planar logarithmic potential

$$\Phi = \frac{1}{2} \ln \left(x^2 + \frac{y^2}{q^2} + R_c^2 \right) \quad (1)$$

are useful for illustrating the procedure. In this example, we employ the values $R_c = 0.14$, $q = 0.6$ and $H = -0.3215$ as with the banana orbits in Paper IV. The banana orbits

librate around the central closed banana, so the harmonic oscillator, with actions (J_x, J_y) , is used as H_T . Therefore, we have to map between a straight line in toy configuration space ($J_y = 0, y = 0$) and a curved line in target configuration space ($J_2^2 = 0$).

In Fig. 1, three superposed banana orbits are shown. The innermost orbits are not unlike bent versions of the rectangular orbits of the harmonic oscillator; also, their short ends seem to remain perpendicular to the central orbit after bending. This suggests that we move a local Cartesian coordinate frame along the closed orbit, and determine the point transformation from the local frame to the global one and vice versa. After this, we define a second point transformation that transforms between our new local coordinate system and toy configuration space, which will complete the required mapping.

Let the closed target orbit be given by $(x'_0(s), y'_0(s))$, where s parametrizes the orbit trajectory. If the motion is circulating (loop-type), this parameter can be the time. If it is librating, s can be the path length. In the following, the subscript ‘ s ’ will denote differentiation with respect to s . We define the generalized velocity, tangent to the orbit, as $v_0 \equiv (x'_{0,s}, y'_{0,s})$. The ‘speed’ $v_0 \equiv |v_0|$ is always non-zero also for librating motion because of the choice of s .

Let a be the perpendicular distance from the closed orbit measured from the point parametrized by s : when the y -axis of the local coordinate frame is aligned with v_0 , values on the frame’s x -axis give a (for librating motion, the orbit is traversed only in one direction for this definition). The point transformation between the local (s, a) - and global (x', y') -coordinate systems is then given by

$$\begin{aligned} x' &= x'_0(s) + \frac{y'_{0,s}}{v_0} a, \\ y' &= y'_0(s) - \frac{x'_{0,s}}{v_0} a. \end{aligned} \quad (2)$$

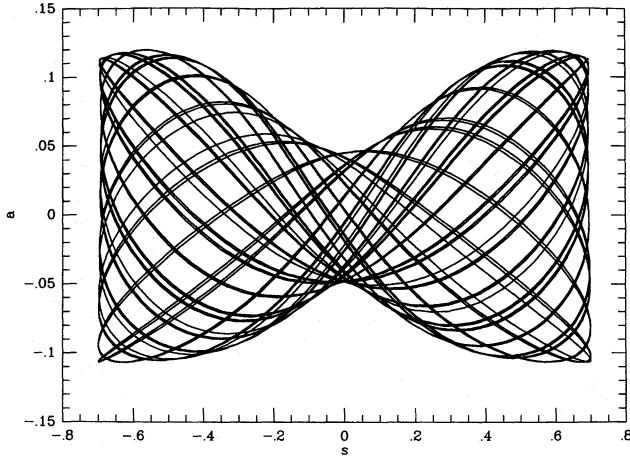


Figure 2. The middle orbit of Fig. 1, shown in (s, a) -space.

In Fig. 2, one of the banana orbits of Fig. 1 is shown in (s, a) -space. (s was chosen to increase from left to right in Fig. 1, so positive a points down.)

The problem with transformation (2) is that, while $(s, a) \rightarrow (x', y')$ is unique, the inverse is not manifestly so. The inverse transformation is now defined as follows: the point (s, a) corresponding to a given (x', y') can be determined by finding where the line with slope $(y' - y'_0(s))/(x' - x'_0(s))$ coincides with the trajectory normal (slope = $-x'_{0,s}/y'_{0,s}$):

$$(y' - y'_0(s))y'_{0,s} + (x' - x'_0(s))x'_{0,s} = 0. \quad (3)$$

The correct solution (s, a) of (3) is the one giving a continuous image in s of motion in H . (Often, but not necessarily always, the value of s is the one corresponding to the (x'_0, y'_0) closest to (x', y') – minimization of this distance gives equation (3).) However, there can be orbits for which a continuous image in s is impossible to achieve with the above choice of a . In such cases, a must be defined in another way. The general principle is to measure s along the closed orbit, and a is some uniquely prescribed measure of the distance from that orbit. There is no general recipe for defining a . It is natural for s - and a -directions to be orthogonal on the parent orbit: then the a -momentum vanishes on it, corresponding to one of the toy momenta on the closed toy orbit.

For a point transformation $x \leftrightarrow \tilde{x}$ between two vectors expressed in arbitrary coordinate systems (see Paper III),

$$\tilde{p}_i = \frac{\partial x}{\partial \tilde{x}_i} \cdot p. \quad (4)$$

From this, one obtains the transformation equations for the momenta in the (s, a) -system. For the closed orbit, $a = 0 = \dot{a}$, and

$$\begin{aligned} p_s &= x'_{0,s} \dot{x}'_0 + y'_{0,s} \dot{y}'_0 = v_0^2 \dot{s}, \\ p_a &= (y'_{0,s} \dot{x}'_0 - x'_{0,s} \dot{y}'_0)/v_0 = 0, \end{aligned} \quad (5)$$

and, along the closed orbit, $\oint p_s ds = \oint \mathbf{p}' \cdot d\mathbf{x}'$. Thus the (s, a) -system can, in its turn, be mapped by a point transformation to a toy system in which one action is zero for the closed orbit image, and the other one equals $\oint p_s ds/2\pi$. When (s, a) and $\tilde{\mathbf{p}} \equiv (p_s, p_a)$ are given, the momenta \mathbf{p}' in Cartesian coordinates can be computed from $\mathbf{p}' = \mathbf{M}^{-1} \tilde{\mathbf{p}}$, where

$$\mathbf{M} \equiv \begin{pmatrix} \partial x'/\partial s & \partial y'/\partial s \\ \partial x'/\partial a & \partial y'/\partial a \end{pmatrix}. \quad (6)$$

Combining (2) with a second point transformation, we have the following transformation chain for a phase-space point w :

$$w_{\text{toy}} \leftrightarrow w_{(s,a)} \leftrightarrow w_{\text{target}}. \quad (7)$$

For orbits of librating type, one can use e.g. the transformation

$$\begin{aligned} x &= g(a)h(s), \\ y &= e(a)f(s), \end{aligned} \quad (8)$$

where (x, y) are the Cartesian coordinates of a toy harmonic oscillator, and the functions e, f, g and h are determined for each orbit. Analogously with the method of Paper III for the small- J' loops, the numerically integrated values for the closed orbit in the target Hamiltonian can now be employed to map an orbit in the harmonic oscillator with $J_x = \oint p_s ds/2\pi, J_y = 0$ into the target one under (8). Specifically, using (4) and considering the closed orbit $a = 0 = \dot{a}$, we obtain (choosing $g(0) = 1$)

$$\frac{dh}{ds} = \frac{p_s}{p_x(h)}, \quad (9)$$

where $p_x(x) = \sqrt{2\omega_x J_x - \omega_x^2 x^2}$ is the x -momentum of the harmonic oscillator with a chosen ω_x . The function $h(s)$ can be solved for either by numerical integration or by directly integrating (9), which yields

$$\frac{h}{2} \sqrt{2\omega_x J_x - \omega_x^2 h^2} + J_x \arcsin h \sqrt{\frac{\omega_x}{2J_x}} = \int_0^s p_s ds. \quad (10)$$

Note that our coordinate system optimizes this transformation in a natural way: the closed orbit determines only $h(s)$ (and even its job can be left to the generating function S if so wished) at $e(0) = 0 = g'(0)$ and a given $g(0)$, while $f(s)$ is arbitrary. Thus e, f, g (and h) can be given as functional series whose coefficients are to be optimized for each constructed torus. When fitting tori with $J_y > 0$, the closed target orbit $(x'_0(s), y'_0(s))$ can be extrapolated in s to cover more of the target configuration space if needed.

Loop-type orbits can be mapped between the isochrone polar toy coordinates and (s, a) much as was done with the small- J' loops. Another possibility, if one wants elongated toy loops instead of circles, is to use the harmonic oscillator in a rotating frame of reference (for its actions and angles see Freeman 1966) as the toy Hamiltonian.

3 TORI FOR BANANA AND FISH ORBITS

3.1 Banana orbits as mildly bent harmonic oscillators

Let us now construct the tori for the orbits in Fig. 1. In this case, the full symmetry of transversal motion about the closed banana orbit $a = 0$ is lost, so the generating function is of the form

$$S(\theta, J') = \theta \cdot J' + 2 \sum_{n>0} S_n(J') \sin[n_1 \theta_1 + n_2 (\theta_2 - \pi/2)], \quad (11)$$

where n_1 runs over all even numbers, and n_2 runs over both even and odd ones. The form $\theta_2 - \pi/2$ is required because the symmetry point in the vertical coordinate y is now only at $\theta_2 = \pm\pi/2$, not at $\theta_2 = 0/\pi$ as well, as in Paper III. Specifically, in the case of a time-reversible orbit, the Fourier series for $S(\theta, J')$ should be written in variables that are zero

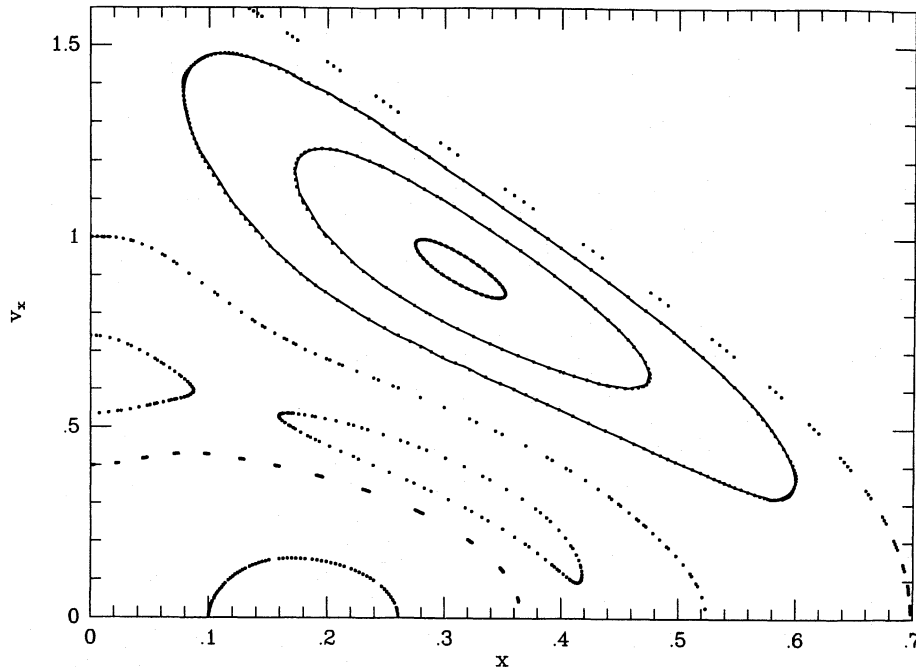


Figure 3. An (x, \dot{x}) surface of section at $R_c = 0.14$, $q = 0.6$ and $H = -0.3215$. The solid lines are sections of constructed tori, and dots are integrated consequents.

at the point $\dot{J} = 0$ (see Paper I); when the symmetry about $x_i = 0$ is lost, $\dot{J}_i = 0$ at $\theta_i = \pm\pi/2$ only.

In Fig. 3, the corresponding (x, \dot{x}) surface of section is shown: sections of the constructed tori are marked as solid lines, and numerically integrated consequents as dots. The actions of the tori are, starting from the outermost one, $J' = (0.4303, 0.0344)$, $(0.4676, 0.0121)$, and $(0.4867, 8.03 \times 10^{-4})$. The actions of the closed orbit are $J' = (0.4880, 0)$. On the island contours of Fig. 3, θ_2 receives all the values in the range $0 \leq \theta_2 \leq 2\pi$, and θ_1 a range of values somewhere inside $0 < \theta_1 < \pi/2$. The functions $e(a)$, $f(s)$ and $g(a)$ in (8) were represented as low-order polynomials, whose coefficients were optimized with the least-squares method as in Papers I–IV using a small initial set of coefficients S_n . After this, a larger final set of S_n was determined using the orbit integration method mentioned in Paper III (see Warnock 1991 and Kaasalainen & Binney 1994b; a summary of the relevant formulae of this method is given in the appendix). The non-linear least-squares method works well, but, since it was possible to employ the orbit integration method in this case, the latter was chosen in order to obtain optimal accuracy and to resolve the power spectrum of the coefficients S_n . The resolution in θ -space was 64×64 for $2\pi \times 2\pi$. As in the examples of the previous papers, the magnitudes of the coefficients decreased in a regular manner with increasing $|n|$.

When constructing tori with the orbit integration method, the form (8) is advantageous as it gives (x, y) explicitly when s and a are known. When using the least-squares construction technique, it is convenient to use the inverse form with functions of x and y to be determined: then there is no numerical root finding anywhere, and the phase-space point w' corresponding to a given trial θ is obtained directly.

The ‘extra’ functions e, f, g in the point transformation (8) are indeed useful; without them, the toy actions vary noticeably

more in θ -space, and a good fit is harder to produce. (8) gives a crude initial distortion of the rectangular harmonic-oscillator box to the bow-tie shapes of banana orbits in (s, a) -space. It is not quite as complete as the elliptic coordinate distortion used for boxes in Paper III. For comparison, (8) was used instead of elliptic coordinates for ordinary boxes, and again it gave a satisfactory initial distortion, although not as good a one as elliptic coordinates would. To be able to use things like elliptic coordinate transformations is basically a stroke of luck; generally, such a priori knowledge is not available.

3.2 Fish orbits as strongly bent harmonic oscillators

If one bends the banana shape even more, it finally crosses itself. A minor-orbit family corresponding to such a shape is the fish family of the singular or near-singular (small R_c) logarithmic potential; a wide fish orbit is shown in Fig. 4, with $q = 0.7$ and $H = 0$ as in Miralda & Schwarzschild (1989; hereafter M&S). The value $R_c = 0.001$ was used to smooth out the central singularity; in practice the orbits look similar to those with $R_c = 0$ in M&S. The fish orbits librate in the same manner as the banana ones, and again the short ends of the orbits seem to retain the perpendicularity to the closed parent orbit. We should thus be able to deal with them as with the bananas.

The fact that an orbit crosses itself does not matter: our local (s, a) -coordinate system separates the two ends of the orbit when straightening it out to the toy configuration space of the harmonic oscillator. In Fig. 5, the orbit of Fig. 4 is shown in (s, a) -space. One can immediately see that the orbit is more complex than the banana ones: instead of the quite symmetric bow-tie shape, it looks more like the Batman logo. (In our new configuration space, one should talk about bow-ties and bats rather than bananas and fishes.) Also, the trajectory densities

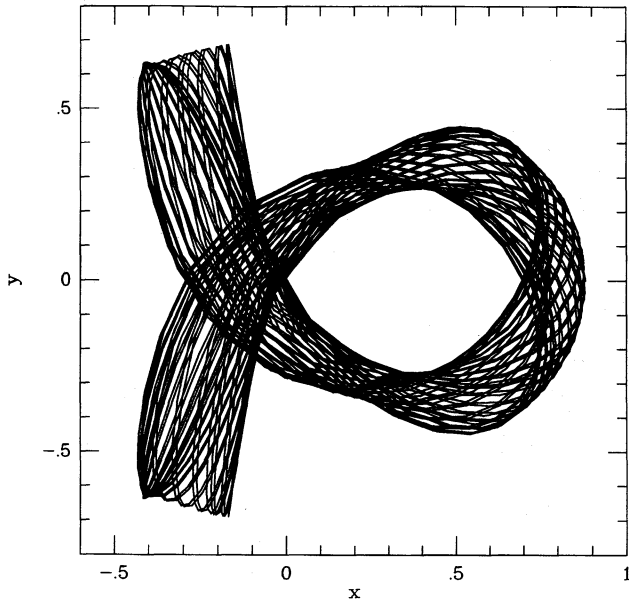


Figure 4. A fish orbit at $R_c = 0.001$, $q = 0.7$ and $H = 0$.

produce ‘folding’ patterns different from the banana orbits. We should thus expect the Fourier series (11) for the generating function S to require more high-order terms than in the banana case. Also, because of the stronger asymmetry, the form (8) for the point transformation appears too restrictive: here one function $e(a)$ does not suffice to modulate $f(s)$ at every s . Hence the more general form

$$\begin{aligned} x &= g(a)h(s), \\ y &= f(s, a) \end{aligned} \quad (12)$$

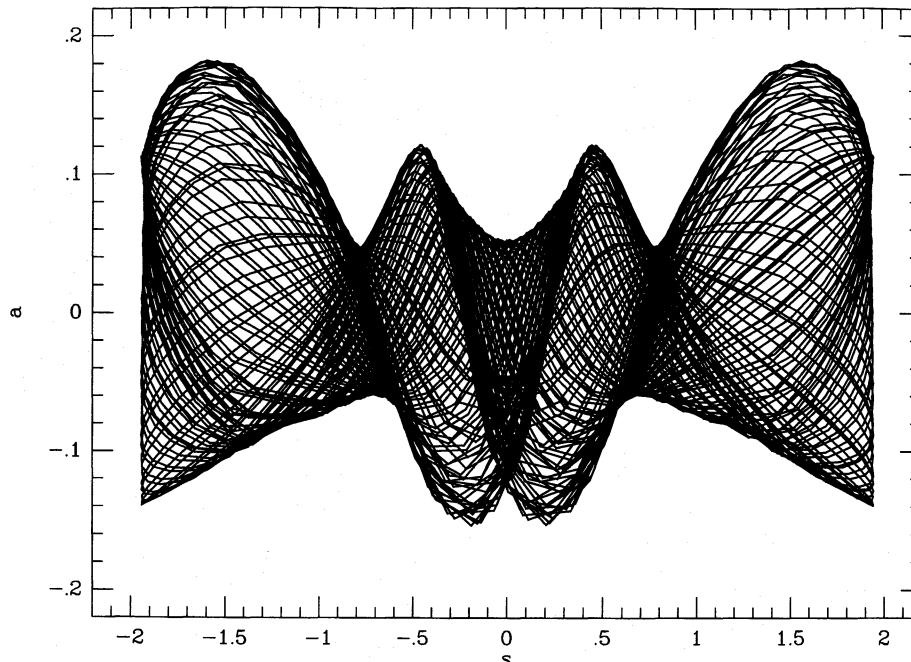


Figure 5. The orbit of Fig. 4, shown in (s, a) -space. s increases anticlockwise in Fig. 4, and a points away from the origin.

was used, with $f(s, a)$ expanded as a bi-polynomial series:

$$f(s, a) = \sum_{i,j} f_{ij} s^i a^j, \quad (13)$$

and the coefficients f_{ij} as well as those of g were optimized as with the bananas above. The form (12) gave somewhat better results than (8).

In Fig. 6, the corresponding (y, \dot{y}) -section is shown with two constructed tori; this section was chosen because it is used in M&S as well (and the islands of each family are somewhat easier to recognize). The actions of the tori are $J' = (1.372, 0.0102)$ and $J' = (1.395, 0.0038)$; the closed orbit is at $J' = (1.409, 0)$. The resolution used was 128×128 ; with 64×64 , sufficient for bananas, the island curves were still quite inaccurate, so there is indeed a lot of high-order power in the coefficients S_n . From Fig. 6 we can thus see that, even though qualitatively a fish orbit can be seen as a strongly bent harmonic oscillator, quantitatively it still has its own strong characteristics, necessitating a long series for S . In this case, the least-squares method for constructing S is not practical: the required set of S_n is many times larger than with the easier box or loop orbits.

4 CONCLUSIONS

The torus-fitting scheme of Papers I–IV has been generalized to cover the case of tori, especially those of a minor-orbit family, around a closed orbit. An additional coordinate system (and the corresponding point transformation) unique to a prescribed closed orbit is necessary for one to be able to deal with orbits of various shapes, especially those crossing themselves. We have applied this approach to two important minor-orbit families in a planar bar, associated with the lowest (1:2 and 2:3) orbital resonances.

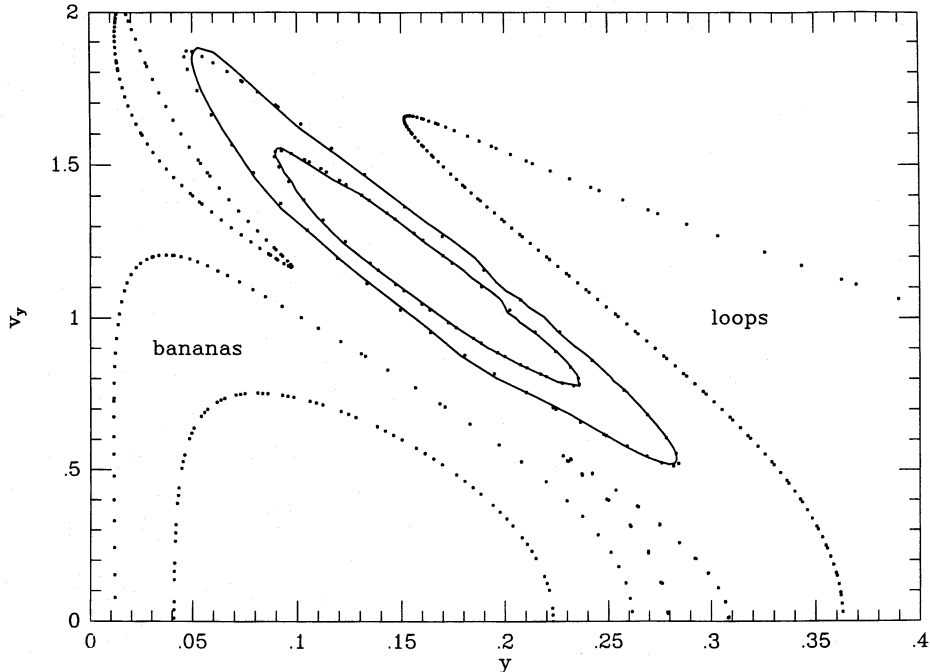


Figure 6. An (y, \dot{y}) surface of section at $R_c = 0.001$, $q = 0.7$ and $H = 0$. The solid lines are sections of constructed tori (the larger island corresponds to the orbit of Fig. 4), and dots are integrated consequents.

An added complication is that the new coordinate system changes with each closed orbit and is therefore no longer universal. Thus, when considering tori at different values of H , one has to move smoothly from one coordinate system to another. In any case, even if one can use universal coordinates in the necessary point transformations (as e.g. in the case of loop orbits at small J_r), the transformations are nevertheless determined for each closed orbit separately.

In our examples, the new coordinate system consisted simply of the closed orbit trajectory and of lines perpendicular to it. There are certainly orbits to which such a system cannot be applied. In such cases, one has to look at each situation separately. One possibility is to distort the target configuration space with simple further transformations (e.g., by expanding or shrinking the coordinate scales); this might mould the orbit into a suitable shape.

How feasible is it to construct tori for a given orbit family? One could say that there are three types of orbits from the point of view of one constructing their tori: orbits for which the more or less automatic schemes of this paper and Papers I–IV can be used; orbits for which torus construction is a ‘sport’ (suitable transformations can be invented, but they apply to each case separately); and orbits that are very difficult to deal with, at least without clairvoyance (these would typically require more general additional canonical transformations than point ones). We are fortunate, in that our examples of orbits of interest in gravitational potentials mostly seem to fall in the first category.

This paper supplements the basic methods and apparatus of Papers I–IV for the torus construction problem. We have shown that an operative scheme is now available that handles the different aspects of the problem, and that the techniques developed can now be applied to, for example, galaxy mod-

elling or perturbative approaches and studies of transition to chaos in stellar dynamics, as well as to problems in other fields of physics.

ACKNOWLEDGMENTS

I am pleased to thank James Binney for useful discussions and comments.

REFERENCES

- Binney J.J., Kumar S., 1993, MNRAS, 261, 584 (Paper II)
- Binney J.J., Spergel D., 1984, MNRAS, 206, 159
- Freeman K., 1966, MNRAS, 133, 47
- Kaasalainen M., 1994, MNRAS, 268, 1041 (Paper IV)
- Kaasalainen M., Binney J.J., 1994a, MNRAS, 268, 1033 (Paper III)
- Kaasalainen M., Binney J.J., 1994b, Phys. Rev. Lett., 73, 2377
- McGill C., Binney J.J., 1990, MNRAS, 244, 634 (Paper I)
- Miralda J., Schwarzschild M., 1989, ApJ, 339, 752 (M&S)
- Warnock R., 1991, Phys. Rev. Lett., 66, 1803

APPENDIX: GENERATING FUNCTION FROM ORBIT INTEGRATION

Warnock (1991) introduced a scheme in which one obtains the coefficients S_n by employing the values taken by \mathbf{J} on a regular grid in θ . This amounts to obtaining the values of \mathbf{J} needed for a discrete Fourier transform (DFT), just as was done directly in the case of Stäckel potentials in Paper I, and on performing DFTs one thus gets the values of nS_n and \mathbf{J}' . As discussed in Kaasalainen & Binney (1994b), this scheme is less general than the least-squares one, but, when applicable, it can give very accurate representations of S .

The set of linear equations is straightforward to obtain. First, recall that the two-dimensional DFT of a 2D function $J(\theta_1, \theta_2)$ is

$$c_{mn} = \frac{1}{MN} \sum_{k=0}^{M-1} \sum_{l=0}^{N-1} J_{kl} \exp \left[-i2\pi \left(\frac{mk}{M} + \frac{nl}{N} \right) \right], \quad (\text{A1})$$

where M, N are the numbers of sampling points in each dimension, and

$$J_{kl} \equiv J(\theta_{kl}) \equiv J \left(\frac{2\pi k}{M}, \frac{2\pi l}{N} \right). \quad (\text{A2})$$

Using c_{mn} as approximations for the coefficients of the 2D Fourier series of J (and identifying the index $M-i$ with the Fourier coefficient index $-i$), we have

$$J(\theta) = \frac{1}{MN} \sum_{k,l} J_{kl} \mathcal{S}_{kM}(\theta_1) \mathcal{S}_{lN}(\theta_2), \quad (\text{A3})$$

where

$$\mathcal{S}_{kM}(\theta) \equiv \sum_m \exp[im(\theta - 2\pi k/M)]. \quad (\text{A4})$$

We use a grid with an even number M of points in a dimension, to be able to employ the symmetries of the system (Warnock uses an odd number, resulting in a slightly different final

expression for \mathcal{S}). The sum over m goes thus from $-(M/2-1)$ to $(M/2-1)$, which can be evaluated as a geometric series, and then the 'halfway' $M/2$ -term is included. Denoting $\tilde{\theta}_{kM} \equiv \theta - 2\pi k/M$, the coefficients $\mathcal{S}_{kM}(\theta)$ are

$$\mathcal{S}_{kM}(\theta) = \frac{\sin(M\tilde{\theta}_{kM}/2) \cos(\tilde{\theta}_{kM}/2)}{\sin(\tilde{\theta}_{kM}/2)}. \quad (\text{A5})$$

From (A3), the grid-point actions J_{kl} can now be solved for by integrating the orbit long enough that there is a point $\theta^{(kl)}$ close to each grid point θ_{kl} . The equation matrix elements $\mathcal{S}_{kM}(\theta_1^{(ij)}) \mathcal{S}_{lN}(\theta_2^{(ij)})$ of (A3) are strongly peaked at kl (when $\theta \rightarrow \theta_{kl}$ for all grid points, the equation matrix becomes an identity matrix). The matrix is therefore sparse and the equations can quickly be solved iteratively (e.g. Gauss-Seidel method). The iteration usually converges robustly, at least when there is a point in each grid cell. Also, the number of iteration steps needed for practical accuracy is usually only a few. Because a matrix element is separated in θ_1 and θ_2 , it is sufficient to store the factors $\mathcal{S}_{kM}(\theta_1^{(ij)})$ and $\mathcal{S}_{lN}(\theta_2^{(ij)})$ separately instead of the big matrix in its entirety.

This paper has been produced using the Royal Astronomical Society/Blackwell Science \TeX macros.